SEMARAK ILMU PUBLISHING

Journal of Advanced Research in Applied Mechanics

Journal homepage:
https://semarakilmu.com.my/journals/index.php/appl_mech/index
ISSN: 2289-7895

Optimizing Dynamic Properties of Dissimilar Plate Structures: A Model Updating and Response Surface Methodology Approach

Rosmaliza Mat Yaacob[1,2], Noor Amzura Abdullah[1], Muhammad Zikri Japri[1], Mohd Shahrir Mohd Sani[1,*]

[1] Advanced Structural Integrity and Vibration Research Group (ASIVR), Faculty of Mechanical and Automotive Engineering Technology, Universiti Malaysia Pahang Al-Sultan Abdullah, 26600 Pekan, Pahang, Malaysia
[2] Faculty of Engineering and Technology, DRB-HICOM University of Automotive Malaysia (DHU), 26607 Pekan, Pahang, Malaysia

ARTICLE INFO

Article history:
Received 28 October 2024
Received in revised form 29 November 2024
Accepted 6 December 2024
Available online 30 December 2024

Keywords:
Joining structures; experiment modal analysis; finite element analysis; model updating; response surface methodology

ABSTRACT

This paper presents a comprehensive exploration of a multi-objective optimization methodology targeting structural parameters to enhance the dynamic properties of dissimilar structures, emphasizing the integration of experimental and numerical modal analysis techniques. In this study, the correlation technique was employed to compare the modal data obtained from FEA with experimental modal analysis, revealing that the CBAR element exhibited the least error rate of 0.86% among the modes, indicating its superior accuracy in simulating bolted structures. Subsequent model updating processes effectively improved the natural frequency predictions, particularly for NF2, leading to an overall reduction in error from 4.65% to 3.08%. Additionally, the RSM approach successfully optimized the structural design variables, achieving a desirability rate of 0.937 and indicating a significant reduction in percentage error. The comparison between the two optimization methods demonstrated their respective strengths, with model updating offering greater precision in setting boundaries, and RSM providing efficient mathematical models for optimization. This study provides valuable insights into the effective enhancement of dynamic properties for dissimilar plate structures, underscoring the significance of both optimization techniques for achieving superior accuracy in structural analysis and design.

1. Introduction

As a result of swift advancements in engineering product development over the past few decades, structural engineers and designers have encountered an increasingly formidable task to integrate dissimilar materials driven by their pursuit of innovative structures or components endowed with precisely tailored properties [1]. This challenge has mainly manifested as a need to adeptly join dissimilar lightweight alloy plate materials, yielding substantial benefits to sectors such as transportation and aerospace [2-4]. This strategic union not only facilitates the development of

* *Corresponding author.*
E-mail address: mshahrir@umpsa.edu.my

https://doi.org/10.37934/aram.130.1.140158

lightweight structures but also holds the promise of helping the transportation and aerospace industries into an era marked by emission reduction and energy conservation endeavors [5-7]. However, this process is fraught with technical difficulties and uncertainties, such as the compatibility, durability, and reliability of the materials and joints [8]. Mechanical joining stands out as an effective method for establishing connections in dissimilar lightweight structures, encompassing techniques such as welding, bolting, and riveting.

Bolted joints have been widely utilized by engineers as a longstanding method for connecting several components. This is mostly because of their advantageous characteristics, including their simplicity in both assembly and disassembly processes, as well as their cost-efficiency. The joints play a vital role in the dynamic behavior of constructed structures, as they contribute to improved structural damping properties and the reduction of structural resonance magnitude [9-11]. Moreover, achieving an appropriate reduction of the structural model for bolted joints is essential, as it can significantly decrease computational time while maintaining accurate predictions. However, their dynamic behavior has not been efficiently predicted and remains incompletely understood [12,13]. The finite element method (FEM) is considered to be an appropriate method for investigating bolted joints due to its ability to precisely and conveniently address the contact problem, which is a crucial aspect of such joints [14]. Finite element analysis (FEA) is particularly well-suited for this purpose. Hence, it is crucial to construct an efficient and optimized finite element (FE) model to precisely forecast the dynamic characteristics of the constructed structure incorporating bolted connections.

The FE method has experienced significant growth in modern structural design and has been extensively utilized in diverse engineering fields owing to its remarkable capabilities and adaptability. In the preceding study, several authors emphasized the significance of accurately simulating near-resonant dynamics in design response calculations. It was observed that even slight modifications in modal parameters, such as damping ratio, natural frequency, and mode shape, can have a substantial impact on the simulation results [15-18]. The year 2021 signifies the commemoration of the eightieth anniversary of the development of the FEM. This approach has emerged as a significant computational tool for conducting engineering design analysis and scientific modeling in several domains, encompassing material and structural mechanics [19]. The FEM has brought about a significant transformation in scientific modeling and engineering design. This advancement has occurred alongside the emergence of a specialized field known as computational mechanics, or computational science and engineering, within the realm of engineering science [20].

Experimental modal analysis (EMA) has garnered significant research interest in the context of investigating structural modifications and advancing structural health monitoring [21-24], and model updates [25-27] through the utilization of modal parameters such as natural frequencies, damping characteristics, and mode shapes [28,29]. Experimental analyses are often characterized by high costs and lengthy time requirements, in contrast to numerical simulations conducted by the FEM, which is widely recognized as a highly versatile numerical approach[30,31]. There are several techniques for estimating modal analyses, which are time domain techniques [32] and frequency domain techniques [33]. Frequency domain methods are extensively utilized in the industrial sector and are characterized by their comprehensiveness, accuracy, and continuous advancements. The modal analyses are estimated by curve fitting the frequency response function (FRF), which is obtained during vibration tests [34,35].

Finite element model updating is a process in which an FE model is adjusted using measured data as precise reference data. This adjustment involves updating certain unknown parameters by reducing discrepancies between experimentally and analytically acquired resonance frequencies and mode shapes [36,37]. Selecting updating parameters is a critical task in the process of model

updating. If a specific parameter does not significantly affect numerical predictions, updating the parameter will lead to a modification in its uncertain value The correction of discrepancies between predictions and results has been achieved through the adjustment of sensitive parameters that required less frequent updates. This phenomenon occurs due to the deliberate selection of sensitive parameters, which aims to minimize the discrepancies found in percentage error [38,39]. Finite element model updating using the MSC Nastran optimization method, namely SOL200, has been employed in several published studies as a means to minimize discrepancies between the predicted results of FEA and the empirical data obtained through EMA [40,41].

In recent years, the Response Surface Methodology (RSM) has emerged as a powerful statistical methodology that has found broad application in the fields of engineering and material science. It is mostly utilized for the optimization and modeling of complex structures through the adoption of Design of Experiments (DoE) methodologies [42,43]. The RSM is capable of effectively considering the interconnection among various design parameters. It determines a clear relationship between design parameters and structural response by utilizing input and output data from finite element software [44]. This approach offers a viable alternative to conducting numerous complete finite element analyses, resulting in significant reductions in computational expenses and analysis time [45]. The RSM is employed as a means of constructing a mathematical model that effectively captures the fundamental relationships between various inputs and corresponding responses [46,47]. Therefore, the final result of the RSM involves the acquisition of optimal factor settings through the optimization of the causality model as the objective function [48,49]. In certain industrial applications or while seeking design optimization, RSM offers engineers a valuable approach to identifying the optimal parameter configurations that optimize process or product qualities.

This paper introduces a multi-objective optimization approach for typical structural parameters aimed at enhancing the dynamic characteristics of dissimilar structures. The study primarily focuses on investigating modal analysis, particularly its application in identifying the dynamic properties of a test structure. To achieve this, EMA and FEA are employed, leveraging numerical prediction methods. The subsequent objective is to apply model update techniques to calibrate an FE model of a dissimilar structure using experimental modal data. Subsequently, the RSM is employed to optimize the structure's design variables, considering a desired objective function. The aims of the comparison are:

i. To examine and illustrate the possibility of enhancing the accuracy and efficiency of modeling and optimization techniques for both approaches.
ii. To provide a framework for researchers

2. Material and methods

2.1 Experimental Modal Analysis

In this study, EMA was conducted on a dissimilar plate structure characterized by a nominal thickness of 2mm and plate dimensions of 380mm x 200mm. The materials employed in this study consist of an aluminum plate, specifically AL6061, and a magnesium plate, denoted as AZ31B. The experimental test structure setup as presented in Figure 1 for dissimilar plates bolted together at the middle (overlap). The plate was discretized into several small elements. The discretization process aimed of the discretization process was to determine the optimal number and placement of measurement points. The estimation of the number of elements was conducted based on the guidance provided by the modal characteristics of the plate, which were derived by finite element analysis. In order to reproduce the free-free boundary condition, the dissimilar plate was hung from the test rig using an elastic cable.

Prior to beginning the experiment, several relevant elements should be taken into account, including the number of accelerometers, measurement points, and excitation techniques. The initial prediction of the dynamic properties of the test plate was initially conducted on the experimental structure in this study. Moreover, the calculated natural frequencies and mode shapes are subsequently employed to determine the appropriate excitation points and measurement locations for the test structure. To ensure a sufficient spatial resolution of global structural mode shapes, the dissimilar plate structure was split into a total of 84 grid points. The selection of the location and measurement points was conducted with meticulous consideration to prevent the presence of nodal points.

The experimental study employed a roving impact hammer and two uni-axial accelerometers to measure the dynamic characteristics of the plate. In the present study, the fixed excitation points were identified as measurement points 45 and 54. The equipment utilized in EMA includes ME's Scope VES, a Data Acquisition system (DAQ), an impact hammer, and a uni-axial accelerometer, as depicted in Figure 2. The extraction of natural frequencies and mode shapes was performed using the curve fitting approach implemented in the ME's Scope VES software.

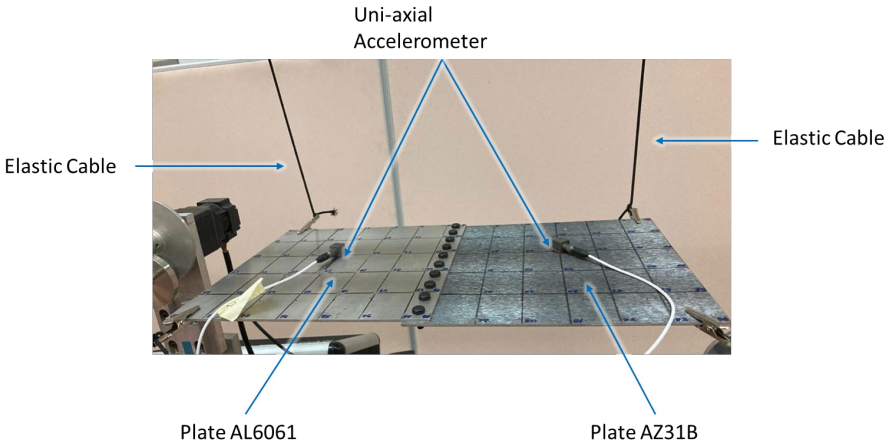

Fig. 1. The experimental modal analysis setup of the plate

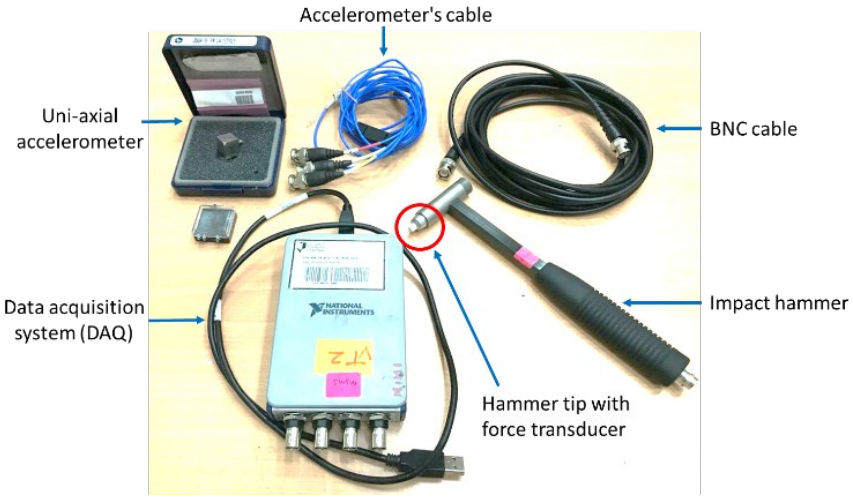

Fig. 2. Tools and instruments used in experimental modal analysis

2.2 Finite Element Modeling

The FE modeling and analysis were conducted using the software program to numerically anticipate the dynamic behaviors of the test structure in this study. There is a scarcity of published research that has undertaken finite element analysis (FEA) on plate structures with bolted joints [50-52]. The 3D CAD model of the dissimilar structure for the bolted joint is depicted in Figure 3. The construction consisted of two distinct plates, namely the AL6061 Plate and the AZ31B Plate, which were interconnected using a total of ten M5 high-speed steel bolts and corresponding nuts. All of the plates possess similar measurements, with a length of 200 mm, a width of 200 mm, and a thickness of 2 mm. The width of overlap between the two plates measures 20 mm.

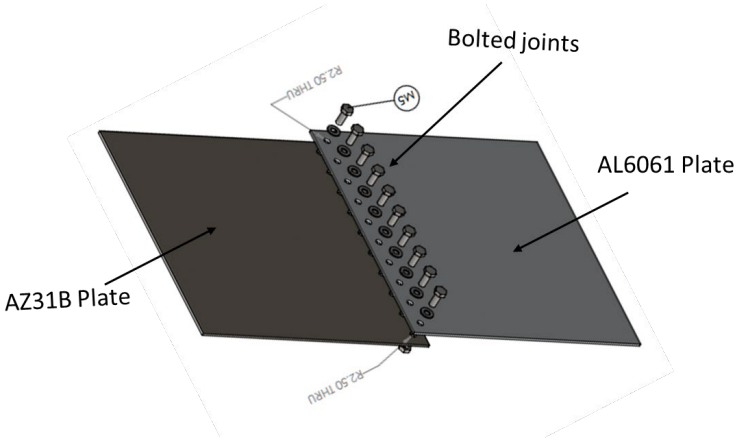

Fig. 3. The CAD model of the plate structure

The FE model of the dissimilar plate structure with joining was developed using NASTRAN software, as represented in Figure 4. This study utilized QUAD4 shell elements to mimic the plate structure. The simulation involved a total of 440 elements and 504 nodes, which encompassed 10 fastening elements. According to the findings of a prior study [53], the chosen joining strategy for this current investigation is CBAR. This decision is based on the recognition that CBAR is the most effective joining strategy, exhibiting the lowest error percentage when compared to the CBEAM and CFAST models. The dimensions of the elements employed for the plate structure were 1 mm, with the element type being a 2D shell element. The overall length of the constructed model measures 380 mm, with a 5 mm gap at the point of overlap.

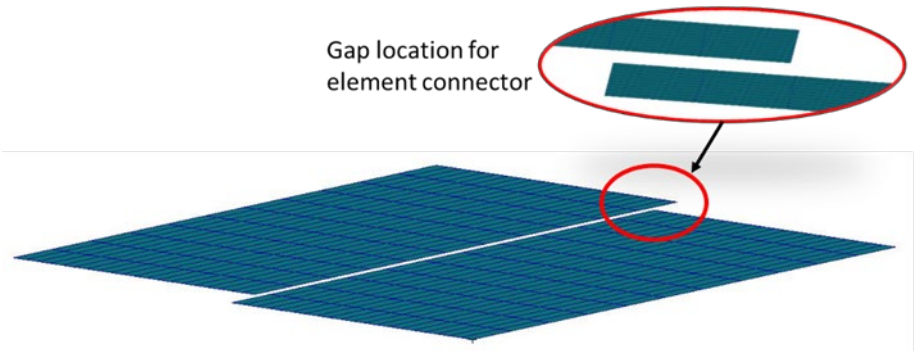

Fig. 4. The FE model of the plate structure

The material properties applied in the FE model are presented in Table 1. After completing the necessary preparations, which include establishing a joint strategy, the modal parameters of the FE model are computed using normal modes analysis from SOL103. The study employed the SOL103 solution sequence to replicate the free-free boundary conditions. This approach ensured that no load, translational, or rotational boundary conditions were imposed on any node within the system [54]. The modal parameters obtained from the calculations were consolidated and presented in Table 2 for the eigenvalues and Table 3 for the eigenvectors of the experimental structure in sub-Topics 3.1 and 3.2.

The CBAR employed an approach of utilizing two grid points in order to enhance the rigidity of the six degrees of freedom associated with each grid point. The elastic axis and shear center of the CBAR were found to be coincident. The material properties utilized for the CBAR joining in the present study include a Young's Modulus of 100 GPa. The displacement components of the grid points consisted of three translations and three rotations.

Table 1
Material properties for structure

Properties	Plate A (AL6061)	Plate B (AZ31B)	Unit
Young's Modulus, *E*	68.9	44.8	GPa
Poisson Ratio, ν	0.33	0.35	-
Density, ρ	2700	1770	kg/m^3

2.3 Finite element model updating

The model updating technique was employed to correct the inaccuracies included in the initially assigned properties that were less precise [55]. The adjustment of parameters was carried out using the MSC Nastran SOL 200 optimization method. Sensitivity analysis approaches were employed to assess the sensitivity of the model parameters, to identify essential parameters, and to prioritize them for adjustment throughout the updating process. The sensitivity coefficient for structural characteristics was calculated using Eq. (1).

$$\boldsymbol{S} = \phi_i^T \left[\frac{\partial \boldsymbol{K}}{\partial \theta_j} - \lambda_i \frac{\partial \boldsymbol{M}}{\partial \theta_j}\right] \phi_i \tag{1}$$

In this context, **S** represents the sensitivity matrix, **K** and **M** refer to the stiffness and FE mass, respectively and ϕ_i is the eigenvector. Additionally λ and θ indicate the eigenvalue and parameter, respectively. Moreover, *i* indicates the eigenvalue corresponding to the *i*th factor and j for the index parameter associated with the *j*th factor. The model update technique was performed by defining an objective function as Eq. (2) to achieve the minimal value when the parameters with a high sensitivity coefficient were acquired.

$$g(x) = \sum_{j=1}^{n} W \left(\frac{\lambda_j^e}{\lambda_j^a} - 1\right)^2 \tag{2}$$

where $g(x)$ denotes the objective function, W represents the positive weighting factor assigned to each mode, and λ_j^e and λ_j^a refer to the natural frequency values obtained from experimental and numerical analysis, respectively. In this study, three parameters have been selected for the sensitivity analysis, namely, Young's Modulus for both the plate and CBAR joining, as illustrated in Figure 5. The

sensitivity coefficient values indicated the significant sensitivity of all parameters. Consequently, all the parameters have been chosen for the process of updating the model.

2.4 Response Surface Method

RSM is a widely used and straightforward approach for analyzing the outcomes of physical experiments and numerical methods, enabling the development of empirically derived models and optimization for response values [56]. The regression model between the optimization objective and the design variables is constructed by RSM using mathematical approaches.

The relationship between the objective value $\boldsymbol{y}$ and the design variables x_1, x_2, …, x_n (where n represents the number of the design variables) in the RSM is described by Eq. (3)

$$\boldsymbol{y}\,(x) = f(x_1, x_2, \ldots\ldots, x_n) + \varepsilon \tag{3}$$

where $f(x)$ denotes a polynomial approximation of (x), while ε represents the residual arising from the discrepancy error between the predicted value and the real value. The polynomial function $f(x)$ is commonly composed of a lower-order degree polynomial, typically assumed to be linear or quadratic. The predicted value is denoted as $\hat{y}$, can be expressed as Eq. (4) when using a quadratic polynomial.

$$\hat{y} = \beta_0 + \sum_{i=1}^{n}(\beta_i x_i) + \sum_{i=1}^{n}(\beta_{ii} x_i^2) + \sum_{i=1}^{n-1}\sum_{j=i+1}^{n}(\beta_{ij} x_i x_j) \tag{4}$$

where $\beta_0, \beta_i, \beta_{ii}, \beta_{ij}$, are the polynomial regression coefficients determined through least-square regression, n is the number of variables, while x_i and x_j are the design variables.

In this study, a Design of Experiments (DoE) methodology was adopted, integrating the application of RSM for comprehensive modeling and analysis, thus providing an efficient framework for optimization through the use of statistical and mathematical techniques. Three numerical factors, namely, A: Young's Modulus AZ31B (E_{AZ31B}), B: Young's Modulus AL6061 (E_{AL6061}), and C: Young's Modulus CBAR (E_{CBAR}), were identified for subsequent optimization using RSM as the input parameters. Each factor was subjected to a three-level factorial design, incorporating variations at low, medium, and high levels, as detailed in Table 2.

Table 2
Level of factor variables

Factor	Codes	Levels		
		Low (GPa)	Medium (GPa)	High (GPa)
Young's Modulus AZ31B (E_{AZ31B})	A	43	45	47
Young's Modulus AL6061 (E_{AL6061})	B	67	69	71
Young's Modulus CBAR (E_{CBAR})	C	90	100	110

The data derived from the simulation was analyzed utilizing Design Expert (DE) version 13, and the significance of the model and response analysis was determined through the application of analysis of variance (ANOVA). ANOVA was employed to assess the equality of the models formulated for each response parameter. To ensure the accuracy and reliability of the findings, it is recommended to subject all simulation outcomes to an ANOVA approach, particularly utilizing the Fisher test (F-test) [57]. Eq. (4) [58] represents the cubic model employed to derive the coefficients of the response parameters based on the variable parameters integrated into the Response Surface

Methodology (RSM). A coefficient is deemed statistically significant when the estimated probability is below the predetermined significance threshold of 5%.

The present study hinges on the utilization of the F-value, which signifies the ratio of the mean square of the model regression to the mean square of the residual. For the analysis to be deemed statistically significant, the F-value must surpass the critical value derived from the tabulated value of the F-Distribution, based on a specific number of degrees of freedom within the model. The correlation between the independent variables and the response variables was evaluated through the visualization of response surface 3D plots.

3. Results and Discussion

3.1 Correlation Between FEA and EMA

The correlation technique has been extensively investigated by multiple scholars in order to compare the modal data obtained from FEA with experimental modal analysis. This comparison aims to determine the level of accuracy with which the generated FE model represents the dynamic behavior of the real structure [59, 60]. The degree of discrepancy between the predictive results and experimental data was subsequently assessed using correlation techniques [61,62]. The selection of the CBAR element as a representation of a fastener joint for the finite element (FE) technique and the updating process was based on its high level of accuracy in simulating a real bolted structure. Additionally, the CBAR element incorporates the latest parameters, making it superior to other joint models [63,64].

The percentage of error for the natural frequency of the FEA using the CBAR element and EMA is shown in Table 2. This study used EMA data as crucial reference points to closely resemble the FEA model. The findings indicate that the initial mode exhibits the biggest error, of 14.57%. This discrepancy can be attributed to multiple factors, including uncertainties in material properties, geometric imperfections, and the existence of manufacturing defects. These factors have a substantial impact on the structural stiffness and damping characteristics of lightweight structures, as noted by Mallareddy [65]. Furthermore, EMA measurements may be influenced by many ambient factors, the configuration of the testing apparatus, and limitations inherent in the instrumentations used.

According to the data presented in Table 3, it is evident that mode NF2 exhibits the lowest error rate of 0.86% in comparison to the remaining modes. The findings indicate that CBAR models possess suitable parameters for model updating in bolted modeling. This is attributed to their enhanced precision in predicting the dynamic behavior of real structures. In order to enhance the correlation between numerical predictions and measured equivalents of bolted models, the adoption of the CBAR model was employed for finite element model updating.

Table 3
Natural Frequency of FEA correlate with EMA data

Mode	Natural Frequency (Hz)		
	EMA	CBAR	Error %
NF1	61.5	70.458	14.57
NF2	199	200.705	0.86
NF3	343	326.83	4.71
NF4	579	593.763	2.55
NF5	633	640.478	1.18
NF6	919	956.061	4.03
Total average error			4.65

3.2 Updated Parameters and Model Properties

FE model updating techniques are purposely to improve the confidence in the analytical analysis. Once the sensitive parameters had been identified through sensitivity analysis, the model updating process was carried out to update the prediction values from FEA with the values obtained from EMA. These updated values were obtained when the less accurate properties definition was corrected into a more optimized value. In this study, three parameters have been selected for the sensitivity analysis, namely, Young's Modulus for both the plate and CBAR joining, as illustrated in Figure 5. The sensitivity coefficient values indicated the significant sensitivity of all parameters. Consequently, all the parameters have been chosen for the process of updating the model.

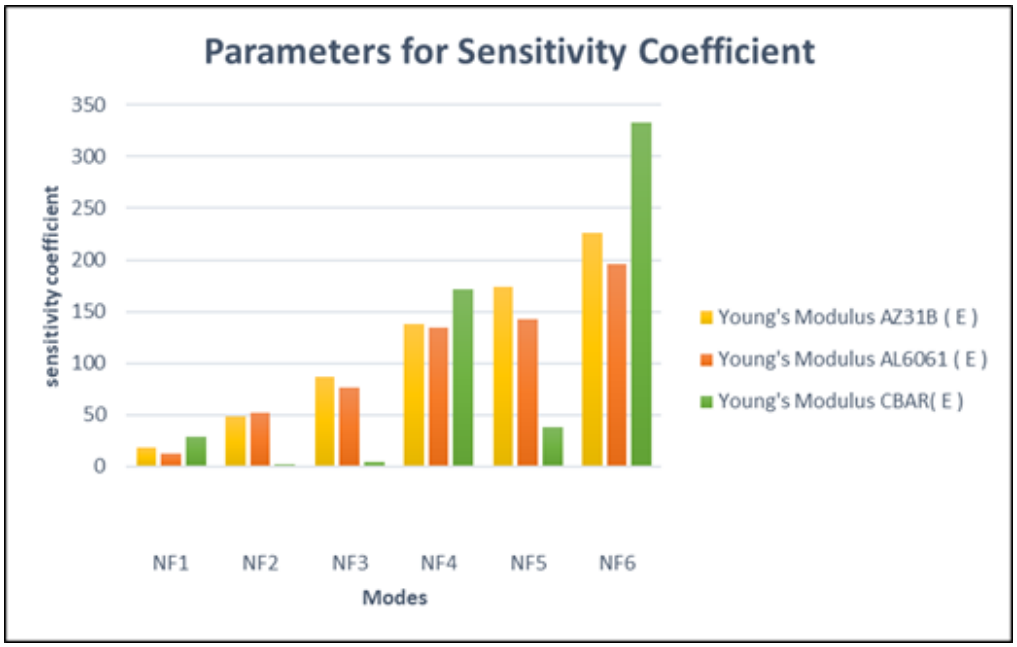

Fig. 5. Parameters for sensitivity coefficient

Table 4 indicates the changes in updated values relative to the initial value for the chosen parameters, as influenced by the design variable. The table indicates that the changes in Young's Modulus for both plate structures exhibit a higher level of sensitivity in comparison to the joining element, mostly due to the assumptions placed within the simulation software. In numerous simulation scenarios, the establishment of the upper and lower boundaries is carried out based on specific assumptions to maintain the simulation's accuracy [66]. When it comes to joining simulations, it is customary to assign higher values to Young's Modulus, as this enhances the rigidity of the element or reduces its deformability. The summary of selected updating parameters is presented in Table 5.

Table 4
Changes in parameter value based on the design variable

Parameter	Initial value (i)	Updated value (u)	Unit	Changes $\lvert(u-i)/i\rvert$
Young's Modulus AZ31B (E_{AZ31B})	44.8	43.46	GPa	0.03
Young's Modulus AL6061 (E_{AL6061})	68.9	69.45	GPa	0.008
Young's Modulus CBAR (E_{CBAR})	100	10	GPa	0.9

Based on the findings presented in Table 5, it is evident that the application of model updating techniques successfully led to the updating of natural frequencies. However, it is important to note that the updated results were obtained with various levels of accuracy. All six modes obtained from the initial FE model were effectively calibrated based on the collected empirical data. The improvement in the adjustment can be shown in column VI, where the total error of the initial FE of 4.65 percent (column IV) was decreased to 3.08 percent. The first mode, NF1 exhibited the most significant inaccuracy, reaching 9.33 percent. However, it is important to note that this result represents a reduction from the initial error value of 14.57 percent. Moreover, the analysis of the cumulative error indicates that the updated findings indicate a decrease in error for 5 values and an increase in error for 1 value, specifically on mode NF3. The inaccuracy exhibited a 0.73 percent increase relative to the initial value of 4.71 percent. The updated value of the parameter in Table 4 will be employed as a replacement for the parameters in the FE model, as it has been validated to closely approximate the experimental structure. In this study, it will be required to compare the results with the RSM to figure out the most effective technique for reducing the discrepancy error in this particular structure.

Table 5
Changes in parameter value based on the design variable

Mode (I)	Natural Frequency (Hz)				
	EMA (II)	Initial CBAR (III)	Error (%) (IV)	Updated CBAR SOL200 (V)	Error (%) (VI)
NF1	61.5	70.458	14.57	67.24	9.33
NF2	199	200.705	0.86	199.47	0.24
NF3	343	326.83	4.71	324.35	5.44
NF4	579	593.763	2.55	571.74	1.25
NF5	633	640.478	1.18	632.25	0.12
NF6	919	956.061	4.03	899.55	2.12
Total average error			4.65		3.08

3.3 Model and Data Analysis

The results pertaining to various response parameters were meticulously scrutinized. The analysis encompasses a detailed evaluation of ANOVA results, focusing on the examination of F-value, R^2, and adjusted R^2 values, alongside the analysis of the significance of variable input parameters on the output parameters. Subsequently, the data underwent analysis using software, leading to the development of an ANOVA table and an appropriate model for the responses.

Table 6 depicts the significance of model terms, based on the ANOVA results derived from the quadratic model for each response. A thorough examination of the table reveals that both E_{AZ31B} (A) and E_{AL6061} (B) have exhibited a significant impact on all parameters, while E_{CBAR} (C) has only demonstrated a discernible effect on the response of Mode NF1 and Mode NF4. The significance of the results is determined by the p-values obtained from the software, where a p-value less than 0.05 or within the 95% confidence interval indicates the significance of the model terms, while a p-value greater than 0.05 suggests insignificance [67].

Table 6
Significance of model terms based on ANOVA results

Response (Mode)	A	B	C	AB	AC	BC	A^2	B^2	C^2
NF1	✓	✓	✓	✓	x	x	x	x	x
NF2	✓	✓	x	x	x	x	x	x	x
NF3	✓	✓	x	✓	x	x	x	x	x
NF4	✓	✓	✓	✓	x	x	✓	x	x
NF5	✓	✓	x	x	x	x	x	x	x
NF6	✓	✓	x	x	x	x	x	x	x

✓ - Significant at 95% confidence interval,
x - not significant at 95% confidence interval

Moreover, the interaction effect of E_{AZ31B} with EA_{L6061} has notably influenced 3 responses, specifically Mode NF1, Mode NF3, and Mode NF4, indicating an acceptable significance within the scope of this study. On the other hand, the interaction effects for E_{AZ31B} with E_{CBAR} and E_{AL6061} with E_{CBAR} have indicated insignificance for all responses within the model. In essence, these results collectively suggest that E_{CBAR}, denoted as the joining component, does not significantly contribute to the overall structural model.

Table 7 presents several statistical parameters derived from the established models. Typically, a higher F-value in ANOVA indicates greater variation between sample means, whereas a lower p-value corresponds to a higher level of significance, providing robust evidence for the significance of the models. The overall significance of the model suggests the significance of all the responses.
The examination of the correlation coefficient (R^2) and adjusted correlation coefficient (Adj. R^2) values serve to assess the precision of the statistical outcomes generated by RSM [68, 69]. Notably, the R^2 and Adj. R^2 for all the models fall within an acceptable range, nearing 1. The magnitude of the R^2 value is viewed as an indicator of the model's adequacy and accuracy in predicting the actual parameter value [70]. The marginal disparity between the R^2 and Adj. R^2 values, less than 0.2, suggest the adequacy of the models.

As indicated in Table 7, the maximum Adj. R^2 is observed for Mode NF1, amounting to 0.9915, while the minimum value is noted for Mode NF6, equalling 0.9365. Based on the correlation coefficient values for each response, the software automatically selected a quadratic model to predict various natural frequency parameters for the dissimilar structure.

Table 7
ANOVA for the response model

Response Mode	Sum of Squares	df	Mean Square	F-value	p-value	R^2	Adjusted R^2
NF1	18.08	6	3.01	506.28*	< 0.0001	0.9935	0.9915
NF2	118.75	3	39.58	192.69*	< 0.0001	0.9617	0.9567
NF3	346.95	6	57.83	352.94*	< 0.0001	0.9906	0.9878
NF4	1038.29	9	115.37	247.42*	< 0.0001	0.9924	0.9884
NF5	1528.64	3	509.55	665.98*	< 0.0001	0.9886	0.9871
NF6	3306.33	3	1102.11	128.81*	< 0.0001	0.9438	0.9365

*indicate the model is significant

The mathematical models for all the responses have been formulated to estimate the respective natural frequency values based on the various input parameters outlined in Eq. (5) through (10), respectively. The variables in these equations are represented in their corresponding units.

NF1 = 77.5979 + (-0.225347) * E_{AZ31B} + (-0.515625) * E_{AL6061} + (-0.0352222) * E_{CBAR} + 0.0122917 * (E_{AZ31B}) (E_{AL6061}) + (-0.00166667) * (E_{AZ31B}) (E_{CBAR})+ 0.00166667 * (E_{AL6061}) (E_{CBAR}) (5)

NF2 = 102.456 + 1.05472 * E_{AZ31B} + 0.732222 * E_{AL6061} + 0.00516667 * E_{CBAR} (6)

NF3 = 377.034 + (-1.39264) * E_{AZ31B} + (-2.58736) * E_{AL6061} + (-0.217889) * E_{CBAR} + 0.06125 * (E_{AZ31B}) (E_{AL6061}) + (-0.00954167) * (E_{AZ31B}) (E_{CBAR})+ 0.00954167 * (E_{AL6061}) (E_{CBAR}) (7)

NF4 = 334.179 + 2.61465 * E_{AZ31B} + 1.25799 * E_{AL6061} + 0.203111 * E_{CBAR} + 0.289792 * (E_{AZ31B})(E_{AL6061}) + (-0.0145417) * (E_{AZ31B})(E_{CBAR}) + 0.015375 * (E_{AL6061})(E_{CBAR}) + (-0.202222) * (E_{AZ31B})^2 + (-0.0980556) * (E_{AL6061})^2 + (-0.00283889) * (E_{CBAR})^2 (8)

NF5 = 321.608 + 4.21889 * E_{AZ31B} + 1.84778 * E_{AL6061} + 0.0267222 * E_{CBAR} (9)

NF6 = 462.596 + 6.13972 * E_{AZ31B} + 2.84611 * E_{AL6061} + 0.0706111 * E_{CBAR} (10)

Figure 6 illustrates the correlation between the predicted and actual values of the parameters. The majority of the data points are observed close to the fit line, indicating a strong correlation between the actual and predicted values. The correlation coefficient values for various parameters suggest the applicability of the developed model in predicting the natural frequency based on the selected material parameters for the dissimilar plate structure. Analysis of the figure reveals that Mode NF1, Mode NF3, and Mode NF4 are positioned closer to the line, demonstrating a higher correlation compared to the other three responses. Moreover, this observation indicates the suitability of these models for the FE data, enabling analysis and prediction of the natural frequency performance.

The effect of the different factors is illustrated through three-dimensional (3-D) response surface plots, segmented data plots represented in Figure 7 to Figure 9. The 3-D response surface curve facilitates mutual comprehension of variable parameters, aiding in the determination of the optimal level for each variable to achieve the maximum response of mode in the natural frequency. Furthermore, the graphs in Figure 7 to Figure 9 aid in identifying the most effective range for all three variable factors. It is evident from the figures that an increase in Young's Modulus corresponds to a decrease in the natural frequency.

Considering the results in Table 6, our discussion primarily focuses on three responses for the 3-D response surface, namely Mode NF1, NF3, and NF4. In Figure 7, the impact of Young's Modulus for both dissimilar plates is more pronounced in the changes of natural frequency, as illustrated in (a), in comparison to the interactions between the Young's Modulus of the plate and the Young's Modulus of the joining component, as depicted in (b) and (c). The peak natural frequency value of 71.9 Hz is notably observed in (a), with a change in value of nearly 2 Hz, whereas the changes are comparatively more subtle in the interactions, at 1.5 Hz and 0.9 Hz, respectively.

Moreover, as illustrated in Figure 8, the maximum peak of the natural frequency value is observed in (a), reaching 333 Hz, with a change in value of nearly 8 Hz, whereas the changes are relatively more subtle in the interactions, at 6.5 Hz and 3 Hz, respectively.

In summary, the modes of natural frequency with distinct material properties reveal significant implications for the update process in FE analysis, facilitating the accurate representation of the actual structure and aiding in the mitigation of vibration effects in lightweight structures.

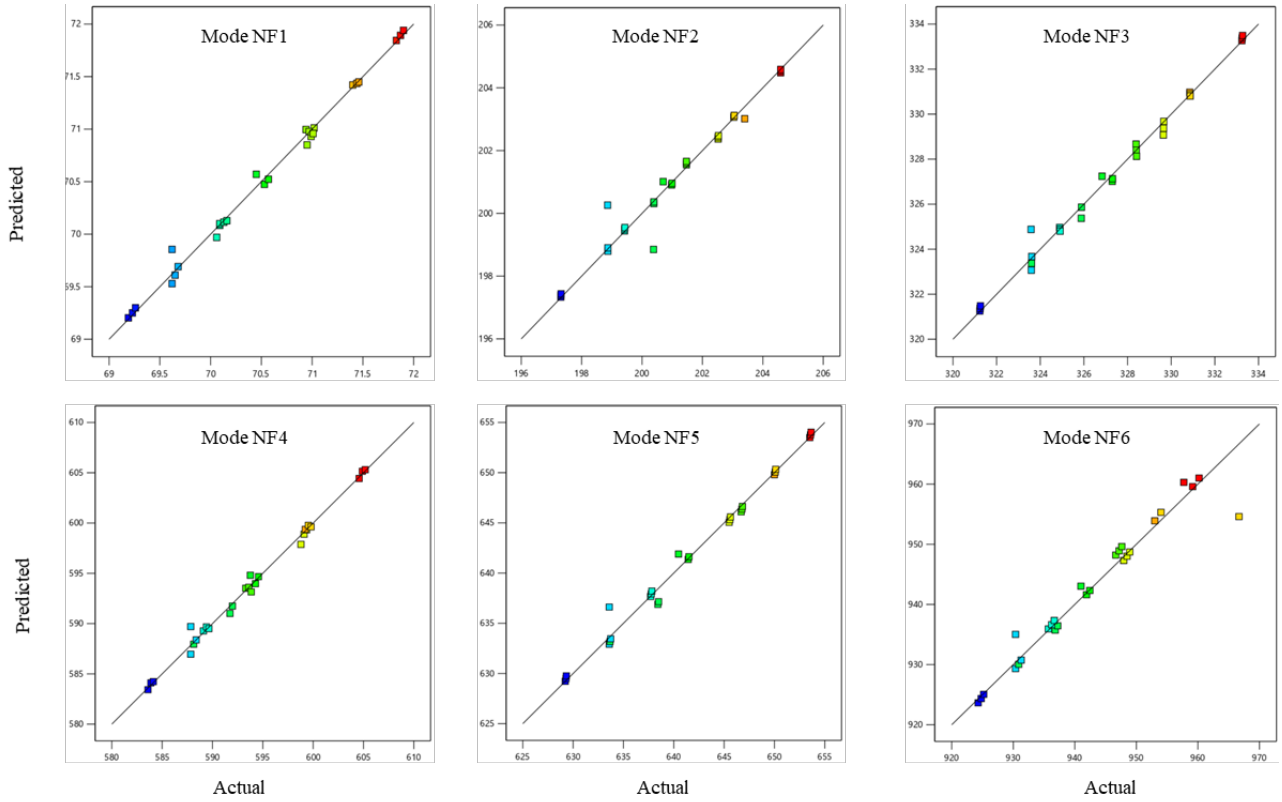

Fig. 6. Simulation vs. predicted values of different responses

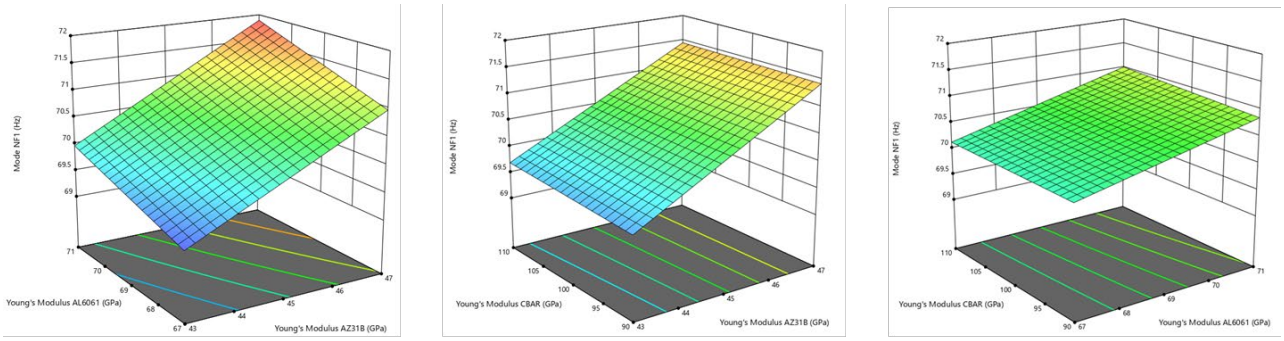

(a) (b) (c)

Fig. 7. Variations of the Mode natural frequency (NF1) vs. effective factor (statistically significant effect)

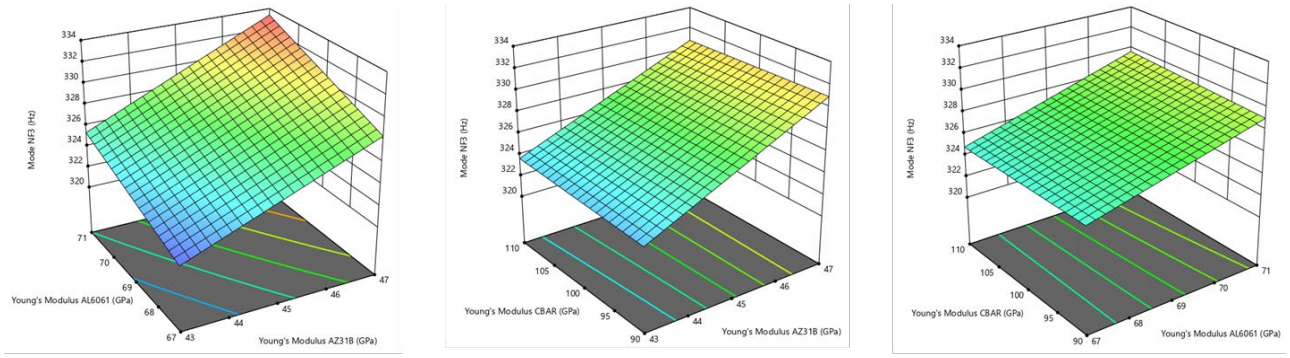

(a) (b)

Fig. 8. Variations of the Mode natural frequency (NF3) vs. effective factor (statistically significant effect)

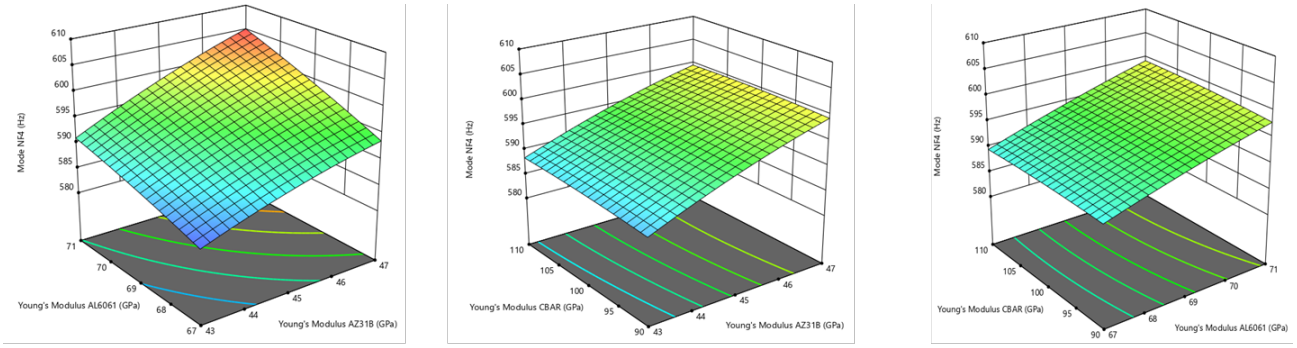

(a) (b) (c)

Fig. 9. Variations of the Mode natural frequency (NF4) vs. effective factor (statistically significant effect)

3.4 Optimization of RSM Results

RSM optimization was performed using input and output response parameters. Young's Modulus AZ31B, Young's Modulus AL6061, and Young's Modulus CBAR are taken as input parameters. An effective mode that was finalized from the comparison between EMA and FEA from the previous study [53], all the six modes of natural frequency are taken as output parameters. Approach, lower and upper limit values of input and response parameters, and optimized parameter value are given in Table 8. During the optimization process, the lower and upper limits of the parameters were determined by RSM. In the approach part, the minimum and value in the range targeted in the response parameters are entered. It is aimed at maximizing the effectiveness of the natural frequency value for the lightweight plate structure. In range approach was chosen for all the main factors while the minimize target was chosen for all the mode responses.

The desirability rate, which is a parameter of the accuracy of the optimization, was determined as 0.937. The fact that the desirability rate value is close to 1 strengthens the suitability of the optimization made [71]. After the optimization, the optimum input parameter values were determined as 43 GPa Young's Modulus AZ31B, 67 GPa Young's Modulus AL6061, and 91.812 GPa Young's Modulus CBAR. Depending on the optimum input parameters, all the responses were found to be very close to the targeted minimum values.

Table 8
Criteria and results of optimization

Parameter	Target	Lower Limit	Upper Limit	Optimized input and response parameter	Unit
A: E_{AZ31B}	In range	43	47	43.00	GPa
B: E_{AL6061}	In range	67	71	67.00	GPa
C: E_{CBAR}	In range	90	110	91.812	GPa
Mode NF1	Minimize	69.19	71.9	69.212	Hz
Mode NF2	Minimize	197.31	204.59	197.342	Hz
Mode NF3	Minimize	321.23	333.27	321.279	Hz
Mode NF4	Minimize	583.59	605.17	583.590	Hz
Mode NF5	Minimize	629.22	653.64	629.275	Hz
Mode NF6	Minimize	924.29	966.68	923.776	Hz

3.5 Comparison of the Optimized Results Between Model Updating and RSM

The final comparison between the two methods, aimed at minimizing the discrepancy error between experimental and numerical data, indicates a notable reduction in the percentage error from the initial CBAR value, as presented in Table 9. The optimization process using SOL200, known

as model updating, yields the lowest percentage error of 3.08, whereas the optimization employing RSM results in a slightly higher percentage error of 3.60. Notwithstanding this difference, the study accomplishes its objective, which is to evaluate the suitability of both optimization methods in reducing the discrepancy error within the lightweight dissimilar structure.

Furthermore, the observed distinctions in the optimization processes can be attributed to the trial-and-error approach employed in setting boundaries for model updating, while for RSM, the levels are established based on predictions derived from the values utilized in FEA. In summary, the comparison underscores the effective implementation of both optimization methods in minimizing errors. While model updating can offer greater accuracy in setting boundaries, it lacks the capability to generate mathematical models, a critical feature provided by RSM in the optimization process.

Table 9
Optimization correlation of natural frequencies for CBAR models

Mode	Natural Frequency (Hz)						
	EMA	Initial CBAR	Error %	Updated CBAR (SOL200)	Error %	Optimization CBAR (RSM)	Error %
NF1	61.5	70.458	14.57	67.24	9.33	69.212	12.54
NF2	199	200.705	0.86	199.47	0.24	197.342	0.83
NF3	343	326.83	4.71	324.35	5.44	321.279	6.33
NF4	579	593.763	2.55	571.74	1.25	583.591	0.79
NF5	633	640.478	1.18	632.25	0.12	629.275	0.59
NF6	919	956.061	4.03	899.55	2.12	923.777	0.52
Total average error			4.65		3.08		3.60

4. Conclusions

In this study, we analyzed and investigated the enhancement of dynamic properties for joining dissimilar plate structures. Experimental and simulation tests were conducted under various conditions, considering factors such as Young's Modulus for both AZ31B and AL6061 plates, as well as the joining CBAR. All material property parameters were measured, leading to the development of a mathematical method correlating these parameters to the considered factors. Subsequently, model updating and Response Surface Methodology (RSM) were applied to optimize the dynamic properties based on sensitivity analysis for the dissimilar plate structure. Based on the study's results, the following conclusions were drawn:

i. The three main factors are interrelated, particularly in the case of Young's Modulus plates, namely E_{AZ31B} and EAL6061.
ii. Mode NF4 exhibits greater accuracy and significance compared to other responses, as evidenced by the interactions and its proximity to the fitted line.
iii. The mathematical model can effectively predict the dynamic properties of the dissimilar plate structure. The adjusted R2 values for mode NF1, NF2, NF3, NF4, NF5, and NF6 models were 0.9935, 0.9567, 0.9878, 0.9884, 0.9871, and 0.9365, respectively.
iv. Both optimization methods effectively reduce discrepancy errors and offer unique advantages in the optimization process. These methods can serve as robust solutions for multi-objective optimization challenges in dynamic properties parameter optimization.

Acknowledgement
The authors would like to thank the Ministry of Higher Education for providing financial support under Fundamental Research Grant Scheme No. FRGS/1/2021/TK0/UMP/02/69 (University reference RDU 210124) and Universiti Malaysia Pahang Al-Sultan Abdullah for laboratory facilities.

References

[1] Smith, Justin D., Dennis H. Li, and Miriam R. Rafferty. "The implementation research logic model: a method for planning, executing, reporting, and synthesizing implementation projects." *Implementation Science* 15 (2020): 1-12. https://doi.org/10.1186/s13012-020-01041-8

[2] Kleinbaum, Sarah, Cindy Jiang, and Steve Logan. "Enabling sustainable transportation through joining of dissimilar lightweight materials." *MRS Bulletin* 44, no. 8 (2019): 608-612. https://doi.org/10.1557/mrs.2019.178

[3] Ji, Shude, Shiyu Niu, and Jianguang Liu. "Dissimilar Al/Mg alloys friction stir lap welding with Zn foil assisted by ultrasonic." *Journal of Materials Science & Technology* 35, no. 8 (2019): 1712-1718. https://doi.org/10.1016/j.jmst.2019.03.033

[4] Gao, Y., Y. Morisada, H. Fujii, and J. Liao. "Dissimilar friction stir lap welding of magnesium to aluminum using plasma electrolytic oxidation interlayer." *Materials Science and Engineering: A* 711 (2018): 109-118. https://doi.org/10.1016/j.msea.2017.11.034

[5] Smith, Christopher J., Ryan J. Kramer, Gunnar Myhre, Kari Alterskjær, William Collins, Adriana Sima, Olivier Boucher et al. "Effective radiative forcing and adjustments in CMIP6 models." *Atmospheric Chemistry and Physics* 20, no. 16 (2020): 9591-9618. https://doi.org/10.5194/acp-20-9591-2020

[6] Khan, Haris Ali, Wei-Ming Wang, Kaifeng Wang, Shengxi Li, Scott Miller, and Jingjing Li. "Investigation of mechanical behavior of dissimilar material FSBR joints exposed to a marine environment." *Journal of Manufacturing Processes* 37 (2019): 376-385. https://doi.org/10.1016/j.jmapro.2018.12.011

[7] Kasaei, M. M., R. Beygi, R. J. C. Carbas, E. A. S. Marques, and L. F. M. da Silva. "A review on mechanical and metallurgical joining by plastic deformation." *Discover Mechanical Engineering* 2, no. 1 (2023): 5. https://doi.org/10.1007/s44245-023-00012-9

[8] Sidhu, Ramandeep Singh, Raman Kumar, Ranvijay Kumar, Pankaj Goel, Sehijpal Singh, Danil Yurievich Pimenov, Khaled Giasin, and Krzysztof Adamczuk. "Joining of dissimilar Al and Mg metal alloys by friction stir welding." *Materials* 15, no. 17 (2022): 5901. https://doi.org/10.3390/ma15175901

[9] El Zaroug, M., F. E. R. H. A. T. Kadioglu, M. Demiral, and D. Saad. "Experimental and numerical investigation into strength of bolted, bonded and hybrid single lap joints: Effects of adherend material type and thickness." *International Journal of Adhesion and Adhesives* 87 (2018): 130-141. https://doi.org/10.1016/j.ijadhadh.2018.10.006

[10] Wall, Mitchell, Matthew S. Allen, and Robert J. Kuether. "Observations of modal coupling due to bolted joints in an experimental benchmark structure." *Mechanical Systems and Signal Processing* 162 (2022): 107968. https://doi.org/10.1016/j.ymssp.2021.107968

[11] Zhang, Hanyu, Lei Zhang, Zhao Liu, Shijie Qi, Yingdan Zhu, and Ping Zhu. "Numerical analysis of hybrid (bonded/bolted) FRP composite joints: A review." *Composite Structures* 262 (2021): 113606. https://doi.org/10.1016/j.compstruct.2021.113606

[12] Cao, Jianbin, and Zhousuo Zhang. "Finite element analysis and mathematical characterization of contact pressure distribution in bolted joints." *Journal of Mechanical Science and Technology* 33 (2019): 4715-4725. https://doi.org/10.1007/s12206-019-0913-x

[13] Zhao, Zhongwei, Bing Liang, Haiqing Liu, and Yongjing Li. "Simplified numerical model for high-strength bolted connections." *Engineering Structures* 164 (2018): 119-127. https://doi.org/10.1016/j.engstruct.2018.02.079

[14] Belardi, Valerio G., Pierluigi Fanelli, and Francesco Vivio. "Theoretical definition of a new custom finite element for structural modeling of composite bolted joints." *Composite Structures* 258 (2021): 113199. https://doi.org/10.1016/j.compstruct.2020.113199

[15] Karaağaçlı, T., and Hasan Nevzat Özgüven. "Experimental quantification and validation of modal properties of geometrically nonlinear structures by using response-controlled stepped-sine testing." *Experimental Mechanics* (2022): 1-13. https://doi.org/10.1007/s11340-021-00784-9

[16] Matsubara, Masami, Akira Saito, and Shozo Kawamura. "Estimation of modal parameters by using the ratios of imaginary to real parts of frequency response functions." *Archive of Applied Mechanics* 91, no. 3 (2021): 1179-1191. https://doi.org/10.1007/s00419-020-01817-w

[17] Omar, R., M. N. A. Rani, M. A. Yunus, M. Rusli, M. A. S. A. Shah, W. I. Izhan, and W. I. Mirza. "Improvement in the accuracy of the dynamic behaviour prediction of a bolted structure using a simplified finite element model and

model updating." In *IOP Conference Series: Materials Science and Engineering*, vol. 1041, no. 1, p. 012051. IOP Publishing, 2021. https://doi.org/10.1088/1757-899X/1041/1/012051

[18] Pai, Anand, Chandrakant R. Kini, and B. Satish Shenoy. "Finite element model for analysis of vibration damping characteristics of isotropic surface structures." *Materials Today: Proceedings* 52 (2022): 518-523. https://doi.org/10.1016/j.matpr.2021.09.270

[19] Liu, Wing Kam, Shaofan Li, and Harold S. Park. "Eighty years of the finite element method: Birth, evolution, and future." *Archives of Computational Methods in Engineering* 29, no. 6 (2022): 4431-4453. https://doi.org/10.1007/s11831-022-09740-9

[20] Asai, Tomoki, Yuki Terazawa, Takashi Miyazaki, Pao-Chun Lin, and Toru Takeuchi. "First mode damping ratio oriented optimal design procedure for damped outrigger systems with additional linear viscous dampers." *Engineering Structures* 247 (2021): 113229. https://doi.org/10.1016/j.engstruct.2021.113229

[21] Wang, Zengwei, Songtao Lei, Long Cheng, Yi Yang, and Lei Ding. "Response prediction for mechanical systems subject to combinational structural modifications." *Journal of Sound and Vibration* 534 (2022): 117019. https://doi.org/10.1016/j.jsv.2022.117019

[22] Zhang, Lin, Tao Zhang, Huajiang Ouyang, Tianyun Li, and Mo You. "Natural frequency assignment of a pipeline through structural modification in layout optimization of elastic supports." *Journal of Sound and Vibration* 561 (2023): 117702. https://doi.org/10.1016/j.jsv.2023.117702

[23] Li, Hedong, Yaozhi Luo, and Demi Ai. "Restoration of electromechanical admittance signature via solving constrained optimization problems for concrete structural damage identification." *Measurement* 214 (2023): 112803. https://doi.org/10.1016/j.measurement.2023.112803

[24] Khazaee, Meghdad, Pierre Derian, and Anthony Mouraud. "A comprehensive study on Structural Health Monitoring (SHM) of wind turbine blades by instrumenting tower using machine learning methods." *Renewable Energy* 199 (2022): 1568-1579. https://doi.org/10.1016/j.renene.2022.09.032

[25] Isnardi, Irma, Edoardo Menga, John E. Mottershead, and Sebastiano Fichera. "An experimental study on the stochastic model updating of a structure with irreducible parameter variability and fixed but unknown hyperparameters." *Mechanical Systems and Signal Processing* 200 (2023): 110597. https://doi.org/10.1016/j.ymssp.2023.110597

[26] Arora, Vikas, Sondipon Adhikari, and Kiran Vijayan. "FRF-based finite element model updating for non-viscous and non-proportionally damped systems." *Journal of Sound and Vibration* 552 (2023): 117639. https://doi.org/10.1016/j.jsv.2023.117639

[27] Abdullah, N. A. Z., M. S. M. Sani, N. A. Husain, M. M. Rahman, and I. Zaman. "Dynamics properties of a Go-kart chassis structure and its prediction improvement using model updating approach." *International Journal of Automotive and Mechanical Engineering* 14, no. 1 (2017): 3887-3897. https://doi.org/10.15282/ijame.14.1.2017.6.0316

[28] Ewins, David J. *Modal testing: theory, practice and application*. John Wiley & Sons, 2009.

[29] Ewins, D. J., B. Weekes, and A. Delli Carri. "Modal testing for model validation of structures with discrete nonlinearities." *Philosophical Transactions of the Royal Society A: Mathematical, Physical and Engineering Sciences* 373, no. 2051 (2015): 20140410. https://doi.org/10.1098/rsta.2014.0410

[30] Balaji, S., S. Dharani Kumar, U. Magarajan, S. RameshBabu, S. Ganeshkumar, Shubham Sharma, Shaimaa AM Abdelmohsen, Indranil Saha, and Sayed M. Eldin. "Comparative analysis of experimental and numerical investigation on multiple projectile impact of AA5083 friction stir welded targets." *Plos one* 18, no. 7 (2023): e0285254. https://doi.org/10.1371/journal.pone.0285254

[31] Hıra, Onur, Senem Yücedağ, Shahrad Samankan, Övgü Yağız Çiçek, and Atakan Altınkaynak. "Numerical and experimental analysis of optimal nozzle dimensions for FDM printers." *Progress in Additive Manufacturing* (2022): 1-16. https://doi.org/10.1007/s40964-021-00241-y

[32] Yu, Xuewen, Danhui Dan, and Liangfu Ge. "Time-domain distributed modal parameter identification based on mode decomposition of single-channel vibration response." *Engineering Structures* 289 (2023): 116323. https://doi.org/10.1016/j.engstruct.2023.116323

[33] Kamali, Soroosh, and Mohammad Ali Hadianfard. "Spectral optimization-based modal identification: a novel operational modal analysis technique." *Mechanical Systems and Signal Processing* 198 (2023): 110445. https://doi.org/10.1016/j.ymssp.2023.110445

[34] De Carolis, Simone, Arcangelo Messina, and Leonardo Soria. "Modal analysis through response-based FRFs: Additional modes for local diagnoses." *Journal of Sound and Vibration* 549 (2023): 117574. https://doi.org/10.1016/j.jsv.2023.117574

[35] Topaloglu, Nezih, and Cevat V. Karadag. "A novel amplitude-FRF based SDOF resonator parameter extraction method." *Journal of Sound and Vibration* 517 (2022): 116551. https://doi.org/10.1016/j.jsv.2021.116551

[36] He, Junzeng, Dong Jiang, Dahai Zhang, Zhenhuan Tang, and Qingguo Fei. "Model updating of rotor system based on the adaptive Gaussian process model using unbalance response." *Journal of Sound and Vibration* 571 (2024): 118006. https://doi.org/10.1016/j.jsv.2023.118006

[37] Bi, Sifeng, Michael Beer, Scott Cogan, and John Mottershead. "Stochastic model updating with uncertainty quantification: an overview and tutorial." *Mechanical Systems and Signal Processing* 204 (2023): 110784. https://doi.org/10.1016/j.ymssp.2023.110784

[38] Shrivastava, Kshitij, Kiran Vijayan, and Vikas Arora. "Experimental identification of dynamic characteristics of welded stiffened structures based on model updating." *Thin-Walled Structures* 184 (2023): 110485. https://doi.org/10.1016/j.tws.2022.110485

[39] You, Chao, Mehdi Yasaee, Shun He, Daqing Yang, Yigeng Xu, Iman Dayyani, Hessam Ghasemnejad et al. "Identification of the key design inputs for the FEM-based preliminary sizing and mass estimation of a civil aircraft wing box structure." *Aerospace Science and Technology* 121 (2022): 107284. https://doi.org/10.1016/j.ast.2021.107284

[40] Fouzi, M. S. M., K. M. Jelani, N. A. Nazri, and Mohd Shahrir Mohd Sani. "Finite element modelling and updating of welded thin-walled beam." *International Journal of Automotive and Mechanical Engineering* 15, no. 4 (2018): 5874-5889. https://doi.org/10.15282/ijame. 15.4.2018.12.0449

[41] Gandhi, Viraj, John Joe, John F. Dannenhoffer, and Hamid Dalir. "Rapid design generation and multifidelity analysis of aircraft structures." *Aerospace Science and Technology* 112 (2021): 106612. https://doi.org/10.1016/j.ast.2021.106612

[42] Pereira, Rhuan José Ribeiro, Fabricio Alves de Almeida, and Guilherme Ferreira Gomes. "A multiobjective optimization parameters applied to additive manufacturing: DOE-based approach to 3D printing." In *Structures*, vol. 55, pp. 1710-1731. Elsevier, 2023. https://doi.org/10.1016/j.istruc.2023.06.136

[43] Sidharthan, S., G. Raajavignesh, R. Nandeeshwaran, N. Radhika, R. Jojith, and N. Jeyaprakash. "Mechanical property analysis and tribological response optimization of SiC and MoS2 reinforced hybrid aluminum functionally graded composite through Taguchi's DOE." *Journal of Manufacturing Processes* 102 (2023): 965-984. https://doi.org/10.1016/j.jmapro.2023.08.013

[44] Wang, Zhiwen, Shouwang Sun, and Youliang Ding. "Fatigue Optimization of Structural Parameters for Orthotropic Steel Bridge Decks Using RSM and NSGA-II." *Mathematical Problems in Engineering* 2022, no. 1 (2022): 4179898. https://doi.org/10.1155/2022/4179898

[45] Mifsud, Darren, and P. G. Verdin. "Surrogate-based design optimisation tool for dual-phase fluid driving jet pump apparatus." *Archives of Computational Methods in Engineering* 28, no. 1 (2021): 53-89. https://doi.org/10.1007/s11831-019-09373-5

[46] Hadiyat, Mochammad Arbi, Bertha Maya Sopha, and Budhi Sholeh Wibowo. "Response surface methodology using observational data: a systematic literature review." *Applied Sciences* 12, no. 20 (2022): 10663. https://doi.org/10.3390/app122010663

[47] Chaurasia, Aman Kumar, Anshul Aggarwal, and Pradeep Khanna. "Mathematical modelling to predict bead geometry in MIG welded aluminium 6101 plates." *Materials Today: Proceedings* (2023). https://doi.org/10.1016/j.matpr.2023.04.145

[48] Khoo, L. P., and C. H. Chen. "Integration of response surface methodology with genetic algorithms." *The International Journal of Advanced Manufacturing Technology* 18 (2001): 483-489. https://doi.org/10.1007/s0017010180483

[49] Alvarez, M. J., L. Ilzarbe, E. Viles, and M. Tanco. "The use of genetic algorithms in response surface methodology." *Quality Technology & Quantitative Management* 6, no. 3 (2009): 295-307. https://doi.org/10.1080/16843703.2009.11673201

[50] Mirza, WI I. Wan Iskandar, MN Abdul Rani, M. A. Yunus, M. A. Ayub, MS M. Sani, and MS Mohd Zin. "Frequency based substructuring for structure with double bolted joints: A case study." *International Journal of Automotive and Mechanical Engineering* 16, no. 1 (2019): 6188-6199. https://doi.org/10.15282/ijame.16.1.2019.8.0470

[51] Wahab, M. A., N. A. Z. Abdullah, M. N. A. M. Asri, and M. S. M. Sani. "Structural dynamic analysis of a frame structure with different sets of bolted joints." In *AIP Conference Proceedings*, vol. 2545, no. 1. AIP Publishing, 2022. https://doi.org/10.1063/5.0103199

[52] Izham, M. H. N., N. A. Z. Abdullah, S. N. Zahari, and M. S. M. Sani. "Structural dynamic investigation of frame structure with bolted joints." In *MATEC Web of Conferences*, vol. 90, p. 01043. EDP Sciences, 2017. https://doi.org/10.1051/matecconf/20179001043

[53] Yaacob, R. M., N. A. Z. Abdullah, and M. S. M. Sani. "Structural model updating of bolted joints in dissimilar material structure." In *AIP Conference Proceedings*, vol. 2545, no. 1. AIP Publishing, 2022. https://doi.org/10.1063/5.0103197

[54] Izham, M. H. N., and M. S. M. Sani. "Model updating of frame structure with bolted joints." In *Journal of Physics: Conference Series*, vol. 1262, no. 1, p. 012023. IOP Publishing, 2019. https://doi.org/10.1088/1742-6596/1262/1/012023
[55] Zárate, Boris A., and Juan M. Caicedo. "Finite element model updating: Multiple alternatives." *Engineering Structures* 30, no. 12 (2008): 3724-3730. https://doi.org/10.1016/j.engstruct.2008.06.012
[56] Korondi, Péter Zénó, Mariapia Marchi, and Carlo Poloni. "Response surface methodology." In *Optimization Under Uncertainty with Applications to Aerospace Engineering*, pp. 387-409. Cham: Springer International Publishing, 2020. https://doi.org/10.1007/978-3-030-60166-9_12
[57] Balti, Sameh, Abderrahim Boudenne, and Noureddine Hamdi. "Characterization and optimization of eco-friendly gypsum materials using response surface methodology." *Journal of Building Engineering* 69 (2023): 106219. https://doi.org/10.1016/j.jobe.2023.106219
[58] Ardebili, Seyed Mohammad Safieddin, Mustafa Babagiray, Emre Aytav, Özer Can, and Andrei-Alexandru Boroiu. "Multi-objective optimization of DI diesel engine performance and emission parameters fueled with Jet-A1–Diesel blends." *Energy* 242 (2022): 122997. https://doi.org/10.1016/j.energy.2021.122997
[59] Shah, M. A. S., M. A. Yunus, and M. N. Rani. "A comparison of FE modelling techniques of composite structure using MSC Patran/Nastran software." In *AIP Conference Proceedings*, vol. 2545, no. 1. AIP Publishing, 2022. https://doi.org/10.1063/5.0103287
[60] Alkayem, Nizar Faisal, Maosen Cao, Yufeng Zhang, Mahmoud Bayat, and Zhongqing Su. "Structural damage detection using finite element model updating with evolutionary algorithms: a survey." *Neural Computing and Applications* 30 (2018): 389-411. https://doi.org/10.1007/s00521-017-3284-1
[61] Rotondella, Vincenzo, Andrea Merulla, Andrea Baldini, and Sara Mantovani. "Dynamic modal correlation of an automotive rear subframe, with particular reference to the modelling of welded joints." *Advances in Acoustics and Vibration* 2017, no. 1 (2017): 8572674. https://doi.org/10.1155/2017/8572674
[62] Zahari, Siti Norazila, Mohd Shahrir Mohd Sani, Nurulakmar Abu Husain, Mahadzir Ishak, and Izzuddin Zaman. "Dynamic analysis of friction stir welding joints in dissimilar material plate structure." *Jurnal Teknologi* 78, no. 6-9 (2016). https://doi.org/10.11113/jt.v78.9148
[63] Kilimtzidis, Spyridon, Efthymios Giannaros, Athanasios Kotzakolios, Angelos Kafkas, Ralf Keimer, Jan Baucke, Vassilis Kostopoulos, and George Labeas. "Modeling, analysis and validation of the structural response of a large-scale composite wing by ground testing." *Composite Structures* 312 (2023): 116897. https://doi.org/10.1016/j.compstruct.2023.116897
[64] Pak, Chan-gi. "Finite element model tuning using analytical sensitivity values." *Journal of Aircraft* 60, no. 4 (2023): 1105-1117. https://doi.org/10.2514/6.2023-1854
[65] Mallareddy, Tarun Teja, Sarah Schneider, and Peter G. Blaschke. "Advanced Hammer Excitation Technique for Impact Modal Testing on Lightweight Materials Using Scalable Automatic Modal Hammer." In *Topics in Modal Analysis & Testing, Volume 9: Proceedings of the 36th IMAC, A Conference and Exposition on Structural Dynamics 2018*, pp. 211-216. Springer International Publishing, 2019. https://doi.org/10.1007/978-3-319-74700-2_22
[66] Zak, S., C. O. W. Trost, P. Kreiml, and M. J. Cordill. "Accurate measurement of thin film mechanical properties using nanoindentation." *Journal of Materials Research* 37, no. 7 (2022): 1373-1389. https://doi.org/10.1557/s43578-022-00541-1
[67] Jaliliantabar, Farzad, Barat Ghobadian, Gholamhassan Najafi, Rizalman Mamat, and Antonio Paolo Carlucci. "Multi-objective NSGA-II optimization of a compression ignition engine parameters using biodiesel fuel and exhaust gas recirculation." *Energy* 187 (2019): 115970. https://doi.org/10.1016/j.energy.2019.115970
[68] Myers, Raymond H., Douglas C. Montgomery, and Christine M. Anderson-Cook. *Response surface methodology: process and product optimization using designed experiments*. John Wiley & Sons, 2016.
[69] Hasan, M. M., M. G. Rasul, M. I. Jahirul, and M. M. K. Khan. "Fast pyrolysis of macadamia nutshell in an auger reactor: Process optimization using response surface methodology (RSM) and oil characterization." *Fuel* 333 (2023): 126490. https://doi.org/10.1016/j.fuel.2022.126490
[70] Prasad, G. Arun, P. C. Murugan, W. Beno Wincy, and S. Joseph Sekhar. "Response Surface Methodology to predict the performance and emission characteristics of gas-diesel engine working on producer gases of non-uniform calorific values." *Energy* 234 (2021): 121225. https://doi.org/10.1016/j.energy.2021.121225
[71] Kocakulak, Tolga, Serdar Halis, Seyed Mohammad Safieddin Ardebili, Mustafa Babagiray, Can Haşimoğlu, Masoud Rabeti, and Alper Calam. "Predictive modelling and optimization of performance and emissions of an auto-ignited heavy naphtha/n-heptane fueled HCCI engine using RSM." *Fuel* 333 (2023): 126519. https://doi.org/10.1016/j.fuel.2022.126519